Catalysis Today 443 (2025) 114964

Contents lists available at ScienceDirect

Catalysis Today

journal homepage: www.elsevier.com/locate/cattod

Sulfured FeMo carbides and nitrides catalysts upgrade extra heavy crude oil quality

Yanet Villasana [a,b,c,*], Joaquin L. Brito [a,b], Miguel Ángel Luis-Luis [c], Franklin J. Méndez [d,**]

[a] Biomass Laboratory, Biomass to Resources Group, Universidad Regional Amazónica IKIAM, Tena, Ecuador
[b] Centro de Química Gabriel Chuchani, Instituto Venezolano de Investigaciones Científicas, Carretera Panamericana Km 11 Altos de Pipe, Caracas 1020A, Venezuela
[c] Facultad Experimental de Ciencias y Tecnología. Universidad de Carabobo, Bárbula, Venezuela
[d] Departamento de Materia Condensada, Instituto de Física, Universidad Nacional Autónoma de México, Ciudad de México 04510, Mexico

ARTICLE INFO

Keywords:
Carbides
Extra-heavy crude oil
FeMo-catalysts
Nitrides
S-removal
Sulfides

ABSTRACT

In the context of the energy transition scenario, effective sulfur management is crucial. Enhancing the quality of extra heavy crude oil (EHCO) through catalytic processes, specifically hydrotreatment, is essential for reducing pollutant emissions like SOx into the atmosphere. Traditional hydrotreatment, utilizing MoS_2-based catalysts typically on Al_2O_3 support, faces challenges with EHCO due to its elevated S and N content, which hampers catalyst efficiency. Metal carbides and nitrides exhibit promising electronic structures that confer resistance to deactivation in the presence of heteroatoms. This study compares the catalytic performances of Fe-promoted Mo sulfides, carbides, and nitrides (FeMoS(C,N)) in the thiophene hydrodesulfurization (HDS) reaction, serving as a model molecule for sulfur removal. Subsequently, we investigate the upgrading of a Venezuelan EHCO in terms of pollutant reduction, API gravity, and feedstock aromaticity. Catalysts were prepared from oxide precursors, varying the (Fe/(Fe+Mo)) atomic ratios (x = 0.00, 0.10, 0.33, 0.50, and 1.00), employing a temperature-programmed reaction protocol. Catalytic upgrading of EHCO was conducted in a stirred batch reactor, and the results were compared with a commercial CoMo-based catalyst. FeMoC(N) outperformed the commercial catalyst in sulfur removal. The elemental composition and nitrogen content of the feed remained constant; however, the sulfur content of asphaltenes decreased. Furthermore, the API gravity of crude oil increased when employing FeMoS and FeMoN catalysts, except with FeMoC, possibly linked to dealkylation reactions and the enrichment of lighter fractions with alkanes. FeMoN increased asphaltene aromaticity, while FeMoC decreased it. These results highlight the promise of FeMoC(N) as catalysts for HDS and upgrading heavy feedstocks.

1. Introduction

Crude oil is expected to maintain its position as the primary global energy source in the years ahead, contributing around 60 % to the total energy supply by 2050, according to the World Energy Outlook 2022 by the International Energy Agency (IEA) [1]. The decline in traditional reservoirs poses a challenge to meeting the demand for oil, necessitating the exploration of unconventional reservoirs like oil sands and heavy crude oil. Currently, the worldwide demand for crude oil stands at approximately 6.6×10^9 m^3 annually, roughly equivalent to 100 million barrels per day [2,3]. This demand primarily driven by the global requirement for liquid transportation fuels, although the IEA anticipates a gradual increase in the petrochemical production's proportional contribution. Notably, almost 85 % of the total consumption of crude oil is accounted for by global oil refining throughput [3]. Consequently, the energy sector remains a major contributor to air pollution, affecting over 90 % of the world's population and causing more than 6 million premature deaths annually [1]. Meanwhile, the global average surface temperature has surpassed pre-industrial levels by about 1.2 °C, leading to heatwaves and other extreme weather events, while greenhouse gas emissions have yet to reach their peak [1]. To contribute to the mitigation of climate change, Europe has implemented regulations to reduce S-content to less than 10 ppm since 2015, while in the US, refineries were required to reduce S-levels in diesel to less than 15 ppm. In accordance with these restrictions, nearly 100,00 tons of HDS catalysts are required annually in refineries and petrochemical industries to

* Corresponding author at: Biomass Laboratory, Biomass to Resources Group, Universidad Regional Amazónica IKIAM, Tena, Ecuador.
** Corresponding author.
E-mail addresses: yanet.villasana@ikiam.edu.ec (Y. Villasana), fmendez@fisica.unam.mx (F.J. Méndez).

https://doi.org/10.1016/j.cattod.2024.114964
Received 12 February 2024; Received in revised form 1 July 2024; Accepted 28 July 2024
Available online 30 July 2024

remove S and other impurities from petroleum [4]. However, conventional catalysts based on Mo sulfides exhibit significant deactivation when processing heavy crude oil, due to elevated levels of metal, sulfur, and nitrogen contents, compounded by the deposition of coke derived from the high content and low stability of asphaltenes [5]. Therefore, research and innovation of alternative and more stable catalysts become a necessity to process these unconventional heavy feedstocks required to meet the world's energy and petrochemical needs.

Transition metal carbides and nitrides (TMCs and TMNs) have been explored in HDT processes, demonstrating good performance and stability [6–11]. Mo and W carbides and nitrides have shown similar or better performance in HDS or hydrodenitrogenation (HDN) activities compared to conventional catalyst [12–14]. Additionally, TMCs and TMNs possess refractory properties and resist sintering at high temperatures, with typical crystal structures including face-centered cubic (fcc), hexagonal close-packed (hcp), or simple hexagonal (hex) structures [15]. TMCs and TMNs have exhibited unique catalytic properties, particularly in reactions involving oxygen-containing molecules [16]. Furthermore, their strong interactions with S and N atoms play a crucial role in heteroatom removal reactions like HDS and HDN [17].

Research has shown that dispersed Ni(Co)Mo carbide and nitride phases on alumina support exhibit greater catalytic activity than reference catalysts such as alumina-supported NiMoS and CoMoS catalysts [18]. Notably, under thiophene HDS reaction conditions, the surface of Mo carbide and nitride particles becomes sulfured [19]. Studies have demonstrated that FeMo carbides and nitrides show promise as catalysts for hydroprocessing, particularly in HDS reactions [17–20]. These catalysts have proven stable under typical hydroprocessing conditions, exhibiting high HDS activity and the ability to replace conventional sulfided Mo catalysts [17,19]. The addition of Co to Mo in bimetallic nitride catalysts has been shown to improve HDS conversion [20], suggesting that FeMo carbides and nitrides hold promise for enhancing HDS reactions in hydroprocessing. Although research on model molecules is abundant, reports on the performance of carbides and nitrides with real feedstocks are scarce. Ramanathan and Oyama tested the catalytic HDS, HDN and HDO of a model liquid feed mixture containing dibenzothiophene, quinoline, benzofuran, tetralin, and tetradecane [21]. They found that carbides and nitrides were active for HDN of quinoline following the order group 6 > group 5 > group 4, while post-reaction analysis of materials suggested tolerance to sulfur. Dolce et al. [22] reported competitive specific activities for molybdenum nitrides and carbides in HDN. The authors suggested that transition metal nitrides and carbides hold promise for improving the efficiency and effectiveness of hydrotreatment processes for real feedstocks. Recently, we reported that NiW catalysts with atomic ratio (Ni/(Ni + W) = 0.50 improved API gravity of a heavy crude oil by reducing S-content and modifying the chemical nature of the crude oil and asphaltenes, as confirmed by the H/C ratio, flocculation threshold, C_{aro}/C_{ali} and H_{aro}/H_{ali} ratios. However, HDN performance was poor [23]. Additionally, our group also found that alumina-supported NiMo carbide and nitride remove sulfur and metal from Maya crude oil [24]. In literature, studies related to the use of FeMo carbides and nitrides as catalysts for upgrading of real feedstocks are scarce.

For these reasons, the objective of this study is to explore the effect of applying FeMo carbides and nitrides as catalyst in the upgrading of an extra heavy crude oil. We analyzed their HDS and HDN performance and demonstrated the effect on crude oil properties and asphaltenes. As a preliminary screening, we analyzed thiophene HDS reactions to understand trends in real feedstocks treatment.

2. Experimental

2.1. Synthesis of oxidic catalysts

Al_2O_3-supported Fe-promoted Mo carbides and nitrides were prepared from oxide precursors by varying the (Fe/(Fe+Mo)) atomic ratios (x = 0.00, 0.10, 0.33, 0.50, and 1.00) using a temperature-programmed reaction protocol and then activated as previously reported [23,24]. The supported oxidic precursors were obtained via the incipient wetness impregnation method using pulverized and sieved alumina pellets with a particle size of 220 μm. Initially, the Mo salt ($(NH_4)_6Mo_7O_{24}{\cdot}4\ H_2O$) was used, followed by the addition of the promoter Fe salt ($FeSO_4{\cdot}7\ H_2O$), resulting in a total of 15 wt% of the oxidic active phase. Before Fe incorporation, the catalysts were dried overnight at 120 °C and then calcined at 500 °C. After the Fe incorporation, the samples were dried overnight at the same temperature and then calcined at 700 °C. The selection of calcination temperatures was based on TGA results (not shown) to ensure the formation of the respective oxides.

2.2. Synthesis of carbides or nitrides catalysts

The oxides precursor was placed in a quartz reactor and exposed to a flow rate of 100 mL/min of a 1:4 vol% CH_4/H_2 mixture for carbides or NH_3 for nitrides. The reactor was heated using a THERMOLYNE model 2100 tube furnace from room temperature to 700 °C at a heating rate of 5 °C/min and kept at the maximum temperature for 2 h. Then, the samples were cooled down under the same reaction atmosphere and finally passivated with a flow of 50 mL/min of a 1 vol% O_2/Ar mixture for 1 h. It is important to note that, for tests with real feedstocks, the catalysts were prepared using cylindrical alumina pellets to facilitate the separation of the catalyst from the reaction products.

2.3. Sulfurization protocol

Either oxides, carbides or nitrides precursors were placed in a Pyrex glass reactor and heated in the furnace previously used. Subsequently, a mixture of CS_2 and H_2, obtained by bubbling a 100 mL/min flow of H_2 through thermostated CS_2 at 0 °C, was passed through the reactor. The temperature of the reactor was then raised to 300 °C at a rate of 5 °C/min and maintained for 2 h. Finally, the samples were cooled to room temperature under the same reaction atmosphere [24].

2.4. Catalysts characterization

X-ray diffraction patterns were obtained using a SIEMENS D5005 diffractometer with Cu-Kα radiation (λ=1.5456 Å) and a Ni filter, scanning between 30 and 80°/2θ with a step speed of 0.02°/s. Phase identification was conducted using the JCPDS library [25]. The morphology and composition of passivated and sulfured carbides and nitrides catalysts, which exhibited significant catalytic performance in thiophene HDS, were assessed using a JEOL model JSM-6390 scanning electron microscope (SEM) coupled to an EDS OXFORD micro-analyzer model 7582. Samples were examined both in powder form and as cross-sections of pellet catalysts, which were placed on graphite stubs and coated with gold to ensure adequate conductivity. The textural analysis was performed using an automatic MICROMETRICS-ASAP 2010 analyzer at liquid nitrogen temperature. Specific surface areas were calculated using the Brunauer-Emmett-Teller multipoint method.

2.5. Catalytic tests

The thiophene hydrodesulfurization (HDS) reactions were conducted to identify the most promising catalysts, which were then employed in the subsequent Extra Heavy Crude Oil (ECHO) upgrading. The used methodology in both kinds of experiments is outlined below.

2.5.1. Thiophene HDS

These reaction tests were performed immediately after the presulfiding treatment described in Section 2.3. The reactor temperature was increased to 400 °C, and H_2 was bubbled as a carrier gas through liquid thiophene, which was at 0 °C using a water/ice bath. Under this condition, the initial concentration of thiophene was 2.27 mol%. The

catalytic activity, expressed as thiophene conversion, was monitored using a VARIAN model 3700 gas chromatograph equipped with a packed PORAPAK-Q80/100 column operating at 170 °C with N_2 as the carrier gas. Once stabilized, the steady-state catalytic activities of each catalyst were determined and reported as pseudo-first-order constants for thiophene disappearance, expressed in units of millimoles of thiophene converted to products per gram of catalyst per minute ($mmol_{thiophene}\ g^{-1}\ min^{-1}$).

2.5.2. EHCO upgrading

The catalytic upgrading was performed using 50 g of EHCO, and 500 mg of catalyst in a stirred 250 mL batch reactor for 4 h at a total H_2 pressure of 1000 psi, a temperature of 320 °C, and a stirring speed of 500 rpm, as reported earlier [23]. The EHCO was a sample of Carabobo crude oil from the Orinoco oil belt, donated by PDVSA-INTEVEP (Venezuela). Catalysts were pre-sulfured *ex situ* following the procedure described in Section 2.3, but the sulfurization time was increased to 3 h, and the flow rate was decreased to 60 mL/min to ensure a longer contact time when treating 2000 mg of sample. The results were compared with those obtained using a commercial $CoMo/Al_2O_3$ catalyst denoted as CCS-2.

Asphaltenic fractions were obtained from raw and hydrotreated crude oil by adding 1:40 vol% of n-heptane, stirring for 6 h, and allowing it to stand for 24 h. Subsequently, the precipitate was filtered and washed with n-heptane in a Soxhlet extractor to isolate the asphaltenes. Solid samples were dried in a Schlenk tube using a glycerin bath at a temperature of approximately 60 °C and stored in amber glass vials under a N_2 atmosphere. The percentage of asphaltenes was calculated based on the initial crude volume, as previously reported [23].

2.6. Crude oil and asphaltenes characterization

The specific gravity of crude oil samples was measured at 20 °C using a RUDOLPH density meter model DDM 2911, which helped determine the specific gravity relative to water at 4 °C (0.999840 g/mL). API gravity values were obtained directly with the same equipment at 15.56 °C (60 °F). A BRUKER Advance 300 MHz Nuclear Magnetic Resonance Spectrometer was used to obtain the ^{13}C- and ^{1}H NMR spectra of crude oil and asphaltene samples, using chloroform as solvent. The C, H, N, and S content in 10 mg of the sample were determined using a FISONS elemental analyzer model EA 1108. The analysis took less than 15 mins and had an absolute precision of less than 0.3 % and an absolute reproducibility better than 0.2 %. The results allowed us to verify changes in S and N contents, as well as in the H/C ratio, which serves as an indicator of the aromaticity of the crude oil. The H/C ratio was calculated as reported earlier [23].

3. Results and discussion

3.1. Catalysts properties

The presence of signals corresponding to the face-centered cubic γ-Al_2O_3 phase (PDF card number 29–0063) was verified in the oxide catalysts (see Fig. 1A), with reflection maxima observed at values of 2θ = 37.64°, 45.83°, and 66.82°, corresponding to the (311), (400), and (440) planes, respectively (Fig. 1A). The diffraction pattern of the monometallic Mo catalyst (atomic ratio Fe/(Fe+Mo) = 0.00) showed no signals attributable to the presence of the orthorhombic MoO_3 phase. In contrast, the corresponding Fe monometallic catalyst (atomic ratio Fe/(Fe+Mo) = 1.00) displayed reflection maxima at values of 2θ = 33.23°, 35.71°, and 54.2°, corresponding to the (104), (110), and (116) planes, respectively, of the Fe_2O_3 phase (PDF card number 84–0307), which crystallizes in the hexagonal system with a rhombohedral cell. For the bimetallic catalysts (atomic ratios Fe/(Fe+Mo) = 0.10, 0.33, and 0.50), no evidence of any of the previously mentioned monometallic oxidic phases could be found, nor of a bimetallic phase of iron oxide and

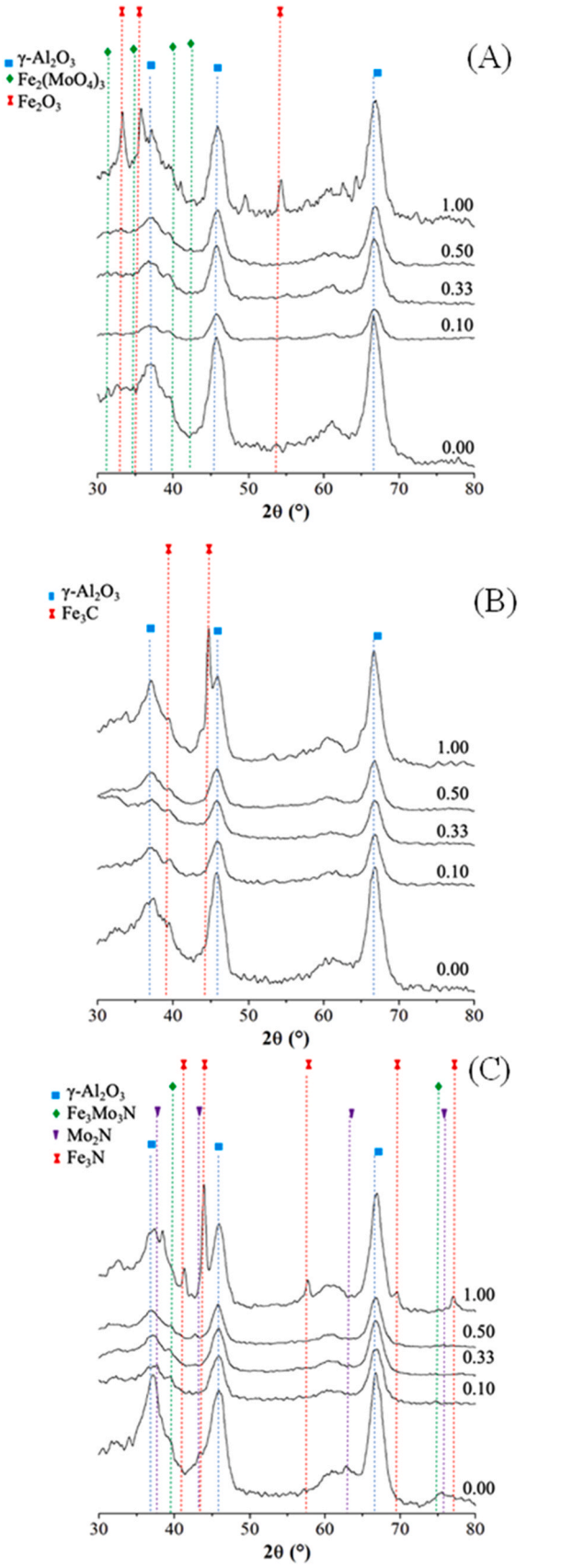

Fig. 1. XRD patterns for the mono- and bimetallic FeMo oxides (A), FeMo carbides (B), and FeMo nitrides (C) catalysts.

molybdenum (or iron molybdate) type (PDF card number 35–0183). This revealed only signals of the support, likely due to the low content of the active phase or highly dispersed particles on the support [18,26–30].

XRD patterns of carbides and nitrides catalysts confirmed that alumina signals prevailed after thermal treatments (Figs. 1B and 1C). The monometallic Mo catalyst showed no signs of the presence of hexagonal Mo carbide (PDF card number 01–1188) or the oxide (Fig. 1B). However, the iron monometallic catalyst exhibited peaks attributable to the Fe_3C phase, with diffraction maxima at values of $2\theta = 37.76°$ and 43.77°, corresponding to the (121) and (102) planes, respectively, of the primitive orthorhombic iron carbide phase (PDF card number 72–1110). This structure conforms to the periodic trends described [31,32], where late metals tend to form structures of the M_3X and M_4X type, indicating a possible rejection of the inclusion of C in the structure by the metal and, consequently, a decrease in the stability of the corresponding carbide. Furthermore, no signs of the presence of a mixed bimetallic phase, such as η-Fe_3Mo_3C, were observed (PDF card number 47–1191). In contrast, the nitrides catalysts exhibit signals at values of $2\theta = 37.70°$, 43.04°, 62.50°, and 75.34°, associated with the planes (112), (200), (220), and (312), respectively, attributable to the Mo_2N phase (PDF card number 75–1150), which crystallizes with a body-centered tetragonal structure (Fig. 1C). This phase conforms to the structure of early transition metal nitrides, which tend to arrange in structures of the MX and M_2X type. On the other hand, the monometallic Fe nitride showed reflection maxima at values of $2\theta = 41.05°$, 43.52°, 63.86°, and 76.50°, associated with the planes (002), ($\bar{1}$ $\bar{1}$ 1); ($\bar{2}$ $\bar{1}$ 1) y ($\bar{1}$ $\bar{1}$ 3) of the hexagonal phase Fe_3N (PDF card number 73–2101), whose structure follows the periodic trend discussed for the corresponding carbide, thus suggesting a decrease in stability. In the bimetallic catalysts, signals indicating the presence of a FeMo phase were found. This phase crystallizes in the face-centered cubic system, with reflection maxima observed at values of $2\theta = 39.87°$ and 74.14°, corresponding to the (442) and (555) planes, respectively, of the Fe_3Mo_3N phase (PDF card number 48–1408). Thus, the trend is evident in which the structures become more complex as we move to the right of the periodic table, as reported elsewhere [31].

To verify the presence of carburized phases in the bimetallic catalysts, specifically the catalyst based on FeMo carbide with an atomic ratio Fe/(Fe+Mo) = 0.10, SEM-EDS analysis was conducted due to its interesting behavior in the thiophene HDS tests (see below). EDS analysis allowed the detection of C, Fe, Mo, Al, and O in both the passivated powder catalyst (Figs. 2A, 2B, and 2C) and the sulfured one (Fig. 2D).

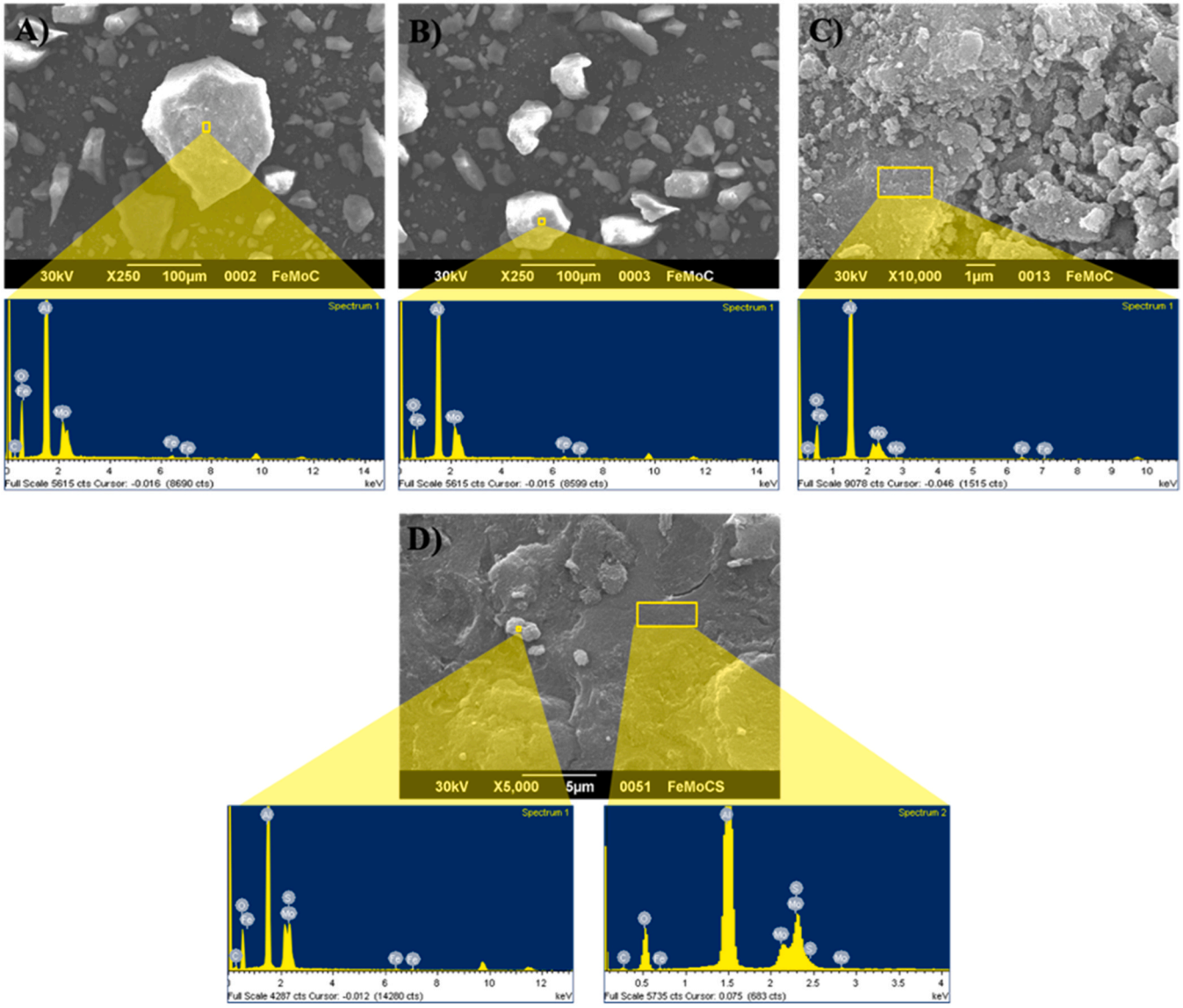

Fig. 2. SEM images and EDS spectra of the FeMo carbides catalyst (Fe/(Fe+Mo) = 0.10): (A, B, C) Powder catalyst before sulfurization process obtained at 250X and 10,000X magnification; and (D) Cross section of a pellet catalyst after sulfurization process obtained at 5,000X magnification.

Furthermore, particles whose composition did not include carbon were found in the powder-passivated catalyst, indicating that part of the oxidic precursor was not converted to the corresponding carbide or simply due to the small area that is analyzed with the technique (Fig. 2B). Additionally, the sulfured pellet effectively showed the presence of sulfur, in addition to the elements already mentioned, which could indicate the formation of some sulfide or carbosulfide species of FeMo (Fig. 2D).

SEM-EDS analysis of the powdered nitrides catalysts showed particles whose composition denoted the presence of Fe, Mo, Al, O, and C (Fig. 3A). The absence of nitrogen could indicate incomplete nitridation of the oxidic precursor. It should be noted that the carbon signal observed may be the result of contamination from the use of carbon tape as a support for the analysis. In addition to the previously mentioned elements, evidence of the presence of nitrogen was found in another section of the sample (see Fig. 3B), confirming the formation of the bimetallic nitride on the alumina matrix (Fig. 3C). The sulfured nitride pellet revealed signals belonging to sulfur, which could indicate the formation of some FeMo sulfide or nitro-sulfide species.

The experimental values corresponding to the atomic ratio obtained by EDS for these FeMo carbide and nitride samples are higher than the nominal value (Fe/(Fe+Mo) = 0.10) in the case of the passivated catalysts, denoted as FeMoC and FeMoN in Table 1. This discrepancy may be due to the segregation of forming monometallic Fe oxides, carbides, or nitrides, which increases the amount of Fe detected during the elemental analysis. In contrast, in the sulfured pellet catalysts, the nominal value and the experimental value agree. Finally, the C and N content remains practically constant even after sulfurization process, both in carbides and nitrides, which suggests the stability of the active phase under sulfiding conditions. However, the values given in Table 1 should be considered as a semi-quantitative compositional analysis which alone is insufficient to provide information on active phases and crystalline structures. For this purpose, it is necessary to apply more advanced techniques such as High-Resolution Transition Electron Microscopy (HRTEM).

Table 2 shows a decrease in the specific surface area (S_{BET}) of the passivated carbides and nitrides catalysts compared to the 246 m^2/g obtained for the Al_2O_3 support. It is well known that the S_{BET} values of a supported catalyst generally decrease as the active phase is added [33]. This decrease is attributed to both a diluting effect of the amount of support and a possible blocking of the porous structure by the supported species. It is also notable that, increasing the Fe content leads to a decrease in this parameter, where the monometallic Fe catalysts (either carbide or nitride) exhibit the lowest values. This phenomenon may be attributed to two reasons: (i) in alumina, Fe ions may migrate towards the support, favoring $Fe^{3+} \leftrightarrow Fe^{2+}$ redox cycles, which induce a sintering effect [34] or (ii) the formation of hercynite spinel structures (Fe-Al_2O_4), where one-eighth of the tetrahedral sites are occupied by Fe^{2+} cations and one-half of the octahedral sites are occupied by Al^{3+} cations, and commonly contain Fe^{3+} cations in octahedral positions. Although the XRD analysis did not detect the formation of these structure types, its formation cannot be completely ruled out.

Table 1
Chemical composition and standard deviation of carbides and nitrides FeMo/Al_2O_3 catalysts with nominal atomic ratio Fe/(Fe+Mo) = 0.10, determined by SEM-EDS.

Catalysts	(Fe/(Fe+Mo)) atomic ratios	S (wt%)	C (wt%)	N (wt%)
FeMoC[a]	(0.22 ±0.01)		(9.0 ± 1.0)	
FeMoCS[b]	(0.10 ± 0.06)	(5.4 ± 0.6)	(13.2 ± 0.9)	
FeMoN[a]	(0.18 ± 0.00)[c]			(5.1 ± 0.5)
FeMoNS[b]	(0.09 ± 0.00)[c]	(3.3 ± 0.3)		(5.0 ± 1.0)

[a] Passivated,
[b] Presulfided,
[c] Only found in one area of the sample.

Table 2
Specific surface area of carbides and nitrides FeMo/Al_2O_3 catalysts.

(Fe/(Fe+Mo)) atomic ratios	Carbides (m^2/g)	Nitrides (m^2/g)
0.00	117	118
0.10	174	193
0.33	186	171
0.50	179	181
1.00	93	99

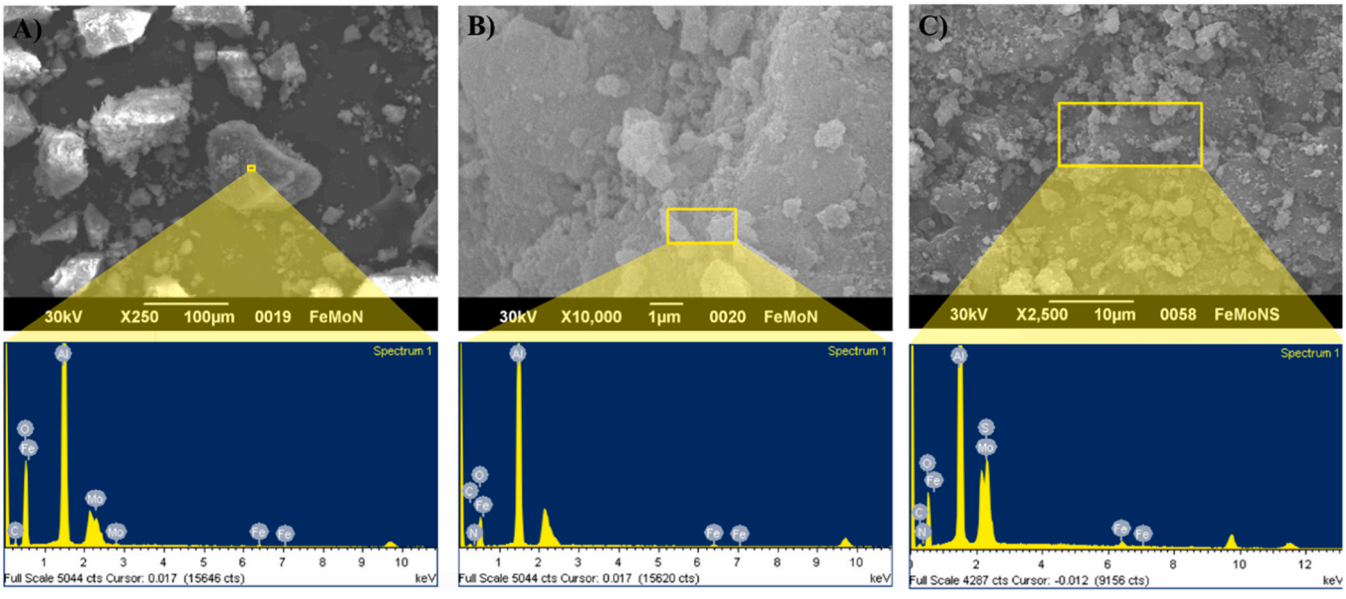

Fig. 3. SEM images and EDS spectra of the FeMo nitrides catalyst (Fe/(Fe+Mo) = 0.10): (A, B) Powder catalyst before sulfurization process obtained at 250X and 10,000X; and (C) Cross section of a pellet catalyst after sulfurization process obtained at 2,500X magnification.

3.2. Catalytic properties

3.2.1. Thiophene HDS performance

When Fe was used as a promoter for the Mo catalysts, it was observed that the FeMo catalyst with an atomic ratio of 0.10 exhibited the highest steady state activity (Fig. 4), despite non-promoted catalyst (Fe/Fe+Mo = 0.00) initially showing the highest activity (inset of Fig. 4). Additionally, the Fe monometallic catalysts presented very low activity. Notably, in the case of the carburized catalyst with an atomic ratio of 0.10, thiophene was rapidly consumed. It is important to note that these measurements were conducted in triplicate, and for catalysts achieving 100 % conversions, the amount of catalyst was progressively reduced, consistently achieving maximum conversion, and only a peak associated with thiophene could be detected during the first injection, a few minutes after the start of the reaction. Therefore, it was concluded that for the FeMo carburized series, the catalyst with an atomic ratio 0.10 exhibits the highest activity. Similarly, for the nitride with the same atomic ratio, it was possible to detect both the initial activity and its activity at 75 min of reaction. After this time, thiophene was completely consumed, allowing for the calculation of minimum activity that this catalyst could have exhibited under these reaction conditions. This activity surpassed that of all other reported activities for this series with different atomic ratios, confirming the maximum in synergy for this atomic ratio for both carburized and nitrided materials. The trends at the beginning of the reaction indicate a decrease in activity with increasing atomic ratio, or, in other words, with higher Fe content, consistent with previous findings for FeW catalysts [35].

The high level of thiophene HDS conversion is related to the capacity of Mo-based carbide and nitride catalysts to activate hydrogen. However, it has been reported that the nitride and carbide particles themselves are not the active phase, but rather a layer of MoS_2 that is formed on the surface. Similar supported CoMo-based catalysts were studied both experimentally and theoretically by DFT during HDS, and authors found that carburization and sulfidation steps reduced the interaction with support, increasing the dispersion of active sites and desulfurization activity [36]. Moreover, under hydrotreating reaction conditions surfaces have been reported to be dynamic and undergo phase transformations. On the other hand, Ramos et al. reported that carbon addition to the edge sites in Co/MoS_2 catalyst, led to a bend of MoS_2 slabs and changes in the morphology increasing the MoS_2 exposure and finally changed activity [37].

3.2.2. Hydrotreating of EHCO characteristics and its asphaltenic fractions

An increase in API gravity was observed in all cases, except when using FeMoCS as catalyst (Fig. 5). Specifically, for this FeMo-based series, it was noted that none of them surpassed the performance of the commercial catalyst, following the trend: CCS > FeMoS > FeMoNS.

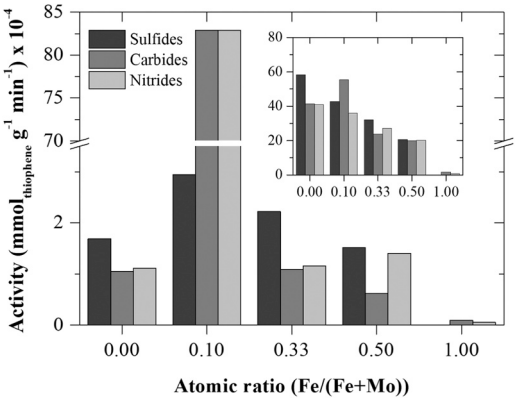

Fig. 4. Effect of atomic ratio on the steady-state catalytic activity and initial activity conditions (inset) for the thiophene HDS of FeMo carbides, nitrides, and sulfides-based catalysts.

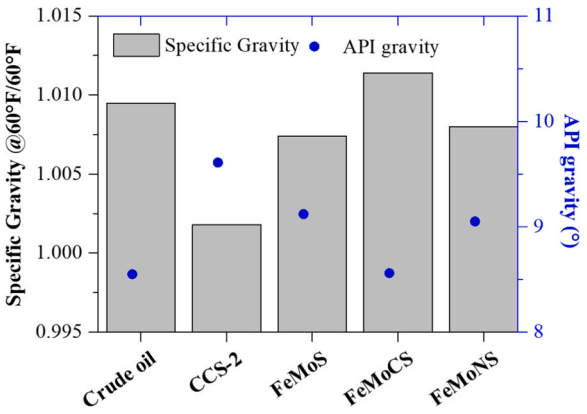

Fig. 5. Specific gravity and API Gravity Elemental of crude oil before and after HT reactions.

Since API gravity of crude oil is related to its specific gravity (the ratio of the density of the crude oil to the density of water under specific conditions), it is important to compare changes in this property during hydrotreatment reactions. In an earlier report we concluded that the specific gravity decreased in all cases with respect to the Maya crude oil, when using Ni(Co)Mo carbides or nitrides as catalyst, following the trend: NiMoN > CoMoN > Commercial Catalysts > CoMoC > NiMoC. Those results were correlated to the high conversion achieved during hydrotreating reactions (by simulated distillation of liquid products) and it was also noted that hydrotreated crude oil samples with low viscosities showed the lowest API gravities [41,42].

Our results aligns with previous results reported by Galarraga et al. [43,44], who reported that the sulfur phase of these catalysts exhibited lower initial activity compared to the CoMo counterpart. However, the FeMo-based catalyst deactivated more slowly. Additionally, it was also found that the presence of a pyrrhotite phase appeared to be necessary for preventing catalyst poisoning and controlling selectivity, although its presence could not be confirmed in our catalytic system, however the presence of such a phase cannot be ruled out.

These catalysts possess remarkable properties suitable for the hydrotreating of heavy crudes and for hydrodemetallization reactions. On the other hand, it is known that the analysis of NMR spectra combined with elemental analysis, either of the crude or of the asphaltenes obtained before and after the hydrotreating reaction, allows for the evaluation of structural changes with the assistance of structural parameter calculations [45]. Elemental analysis revealed that the H/C ratio of the crude oil remains constant during reaction, indicating a predominantly aliphatic character for the Carabobo crude oil (Fig. 6). According to what is known in the literature, it has been established that the higher the H/C ratio the lower the aromatic character of the evaluated charge [45,46]. The NMR results showed a generalized decrease in aromatic H content, probably due to the hydrogenation of aromatic rings and the rupture of naphthenic rings to form simpler aromatic rings with alkyl chains, resulting in a decrease in this parameter.

During EHCO catalytic upgrading, the elemental composition of the feed remained unchanged for all catalyst (Fig. 6A). However, and of the asphaltenes decreased while N remained constant, particularly notable for the HDS performance of FeMo carbides and nitrides, surpassing the removal level achieved with the commercial catalyst (Fig. 6B). Moreover, the API gravity of crude oil increased when FeMoS and FeMoNS catalysts were used, except with FeMoCS (Fig. 5), which could be attributed to dealkylation reactions and enrichment of lighter fractions with alkanes, as supported by NMR analysis (Fig. 7). NMR results also revealed that FeMoNS increased the asphaltenes aromaticity while FeMoCS decreased it. The results indicate that these catalysts are predominantly hydrogenating, but with a hydrocracking component, involving the conversion of naphthenic systems into simpler aromatic

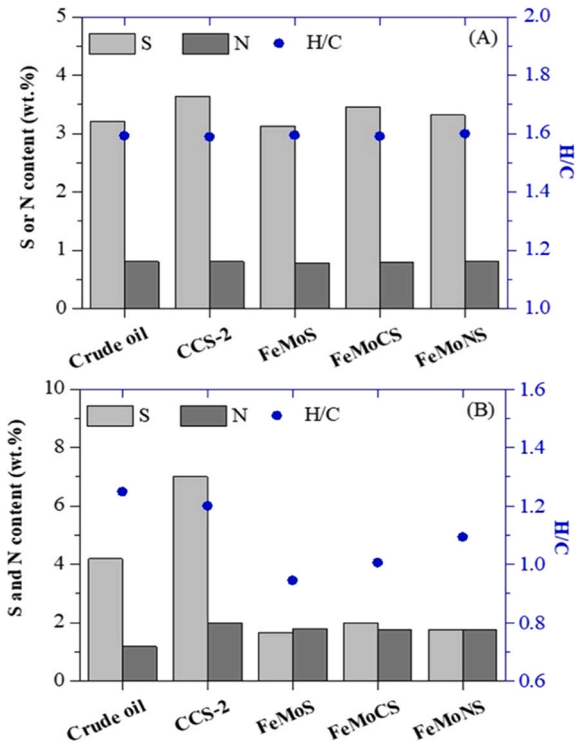

Fig. 6. Elemental analysis of crude oil (A) and asphaltenes (B) after HT catalytic reactions.

molecules and dealkylation of aromatic rings, resulting in an increase in the aromatic C content. This could explain the lower H_{aro} content and higher C_{aro} content found with FeMoCS, according to NMR results. Similar trends were found with $NiMoC/Al_2O_3$ catalyst during aromatics hydrogenation of coal-derived liquids [47].

Fe is generally considered a poor promoter compared to Ni and Co in Mo-based catalysts. However, it has been suggested that, depending on the preparation method, Fe can act as a good promoter of Mo in hydrodesulfurization reactions [38]. Moreover, there is evidence suggesting electron transfer from Mo to Fe, leading to a slight enrichment of electron density around the Fe atom. Nevertheless, the specific location of these electrons remains uncertain. These findings are consistent with previous studies using Mössbauer spectroscopy, which revealed the formation of a new phase (rather than separate Mo and Fe sulfides) in Fe-Mo sulfide mixtures, with an enrichment of d electrons at the Fermi level [39,40]. Previous research has indicated that Fe-promoted Mo catalysts, either bulk or supported on both alumina and carbon, exhibit maximum synergistic effect at atomic ratios around 0.25 and 0.30 [39, 40]. This effect was attributed to the formation of a mixed FeMo sulfided phase, which was confirmed by differences in the work function of the materials through Kelvin probe atomic force microscopy [39,40]. This sulfided mixed phase could not be identified in our catalytic system, however, it is likely that after sulfidation a mixed phase was formed from the mixed oxide (reported and analyzed in the previous chapter). According to the results found by these authors, regarding the distribution of the products obtained, it was possible to define that the catalysts supported on carbon had a material with a hydrogenating character, while those supported on alumina were more hydrogenolyzing. The reasons for this behavior lie in the weak interaction of Mo with the carbon support, which allows a higher degree of stacking (type II active sites), while the strong interaction with alumina favors

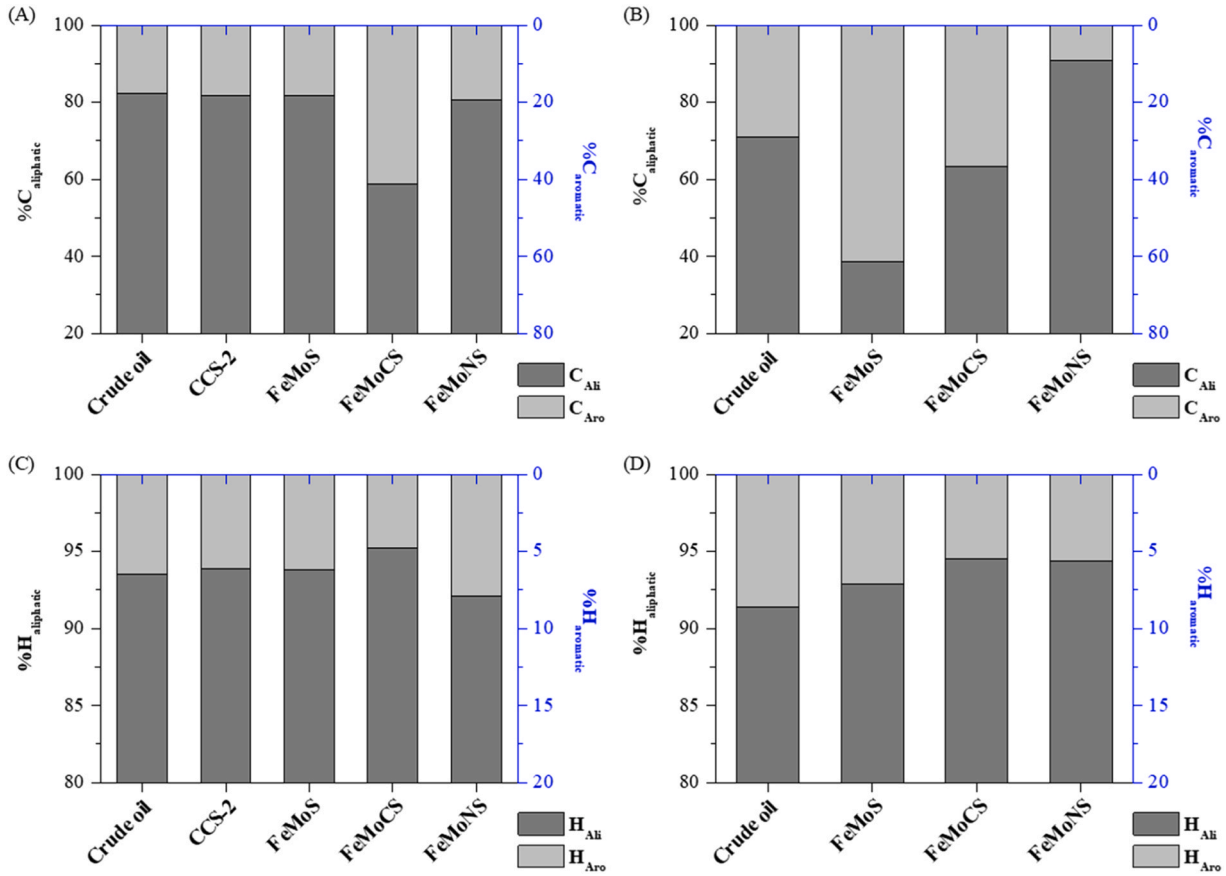

Fig. 7. Aromatic and aliphatic carbon and hydrogen content present in Carabobo crude (A, C) and asphaltene (B, D), before and after HT with FeMo-based catalysts.

more type I active sites (lower degree of stacking), which decreases the routes for HYD to take place. On the other hand, the acidity of alumina itself (Brönsted acidity) rather favors the hydrogenolysis step. Such an effect should be observed to a lesser extent for NiMoS-based catalysts because their activity is less support-dependent.

FeMo carbides were previously studied by Puello-Polo and Brito, who supported them on a carbonaceous matrix and used them as catalysts in thiophene HDS, as discussed in the introductory chapter [48–50]. These authors reported that the behavior of the catalysts, as revealed by TPR and TPR-S analysis, resembled that found for conventional alumina supported catalysts, as reported previously [51,52]. In the earlier report, the first H_2S evolution signal, in the range of 25–300 °C, was attributed to the reduction of S species adsorbed on the CUS, which have been pointed out as responsible for the catalytic performance. Additionally, a linear correlation was also found between the area under the signal and the thiophene HDS activity of the Mo-based activated carbon supported catalysts promoted with Fe, Co, and Ni. According to these results, the authors proposed that the surface of the carbon-supported metal carbide is similar in nature to the surface found on the conventional catalyst and did not rule out the possibility of the formation of a carbosulfide species.

4. Conclusions

The study explores the catalytic performances of Fe-promoted Mo sulfides, carbides, and nitrides in the thiophene hydrodesulfurization reaction, demonstrating the potential of metal carbides and nitrides in resisting deactivation in the presence of heteroatoms. The performance of FeMo carbides and nitrides during thiophene HDS reaction showed a decrease in activity with increasing Fe content, although catalysts with 0.1 of Fe exhibited a synergistic effect surpassing the sulfide activity. Catalysts derived from FeMoC(N) outperform a commercial CoMo-based catalyst in sulfur removal during the upgrading of Venezuelan EHCO, indicating the potential of FeMoC(N) in enhancing the efficiency of hydrotreatment processes. During real feedstock hydrotreating, these catalysts reduced the S content of asphaltenes (FeMoC > FeMoN > FeMoS), but N remain constant, surpassing the performance of commercial catalyst. Moreover, FeMoS and FeMoNS increased API gravity and aromaticity, except with FeMoCS, which was attributed to dealkylation reactions, according to NMR and elemental analysis. FeMo catalysts were identified as predominantly hydrogenating, with a hydrocracking component, transforming naphthenic systems into simpler aromatic molecules and dealkylating aromatic rings, leading to increase in aromatic content. The use of FeMoS and FeMoN catalysts not only improves sulfur removal but also influences the API gravity, feedstock aromaticity, and asphaltene composition of crude oil. FeMoC(N) stands out as a promising catalyst, showcasing potential applications in HDS and upgrading heavy feedstocks.

CRediT authorship contribution statement

Franklin J. Méndez: Writing – original draft, Visualization, Methodology, Data curation, Conceptualization. **Miguel Ángel Luis-Luis:** Supervision, Methodology, Investigation, Funding acquisition, Conceptualization. **Joaquín L. Brito:** Writing – review & editing, Project administration, Methodology, Funding acquisition, Formal analysis, Conceptualization. **Yanet Villasana:** Writing – original draft, Visualization, Software, Methodology, Investigation, Formal analysis, Data curation, Conceptualization.

Declaration of Competing Interest

The authors declare that they have no known competing financial interests or personal relationships that could have appeared to influence the work reported in this paper.

Data Availability

Data will be made available on request.

Acknowledgements

This Special Issue is dedicated to honor the 10th International Symposium on Group V (IV and VI) Elements, a gathering of international researchers, industry, young researchers, and students to help shape the vision of the future for these elements. The authors wish to thank the Instituto Venezolano de Investigaciones Científicas (IVIC, Venezuela) and the Universidad de Carabobo (UC, Venezuela) for their support during the development of this doctoral research. Villasana would also like to thank L'Institut de Recherche pour le Développement (IRD, France) for the training she received to strengthen her skills in writing scientific articles.

References

[1] IEA, World Energy Outlook 2022, Paris, 2022. ⟨https://www.iea.org/reports/world-energy-outlook-2022?language=es⟩.
[2] Oil Market Report - November 2018, Paris (France), n.d. ⟨https://www.iea.org/reports/oil-market-report-november-2018⟩.
[3] A. de Klerk, Transport Fuel (T.M.B.T.-F.E. (Third E. Letcher (Ed.)). Futur. Energy, Elsevier, 2020, pp. 199–226, https://doi.org/10.1016/B978-0-08-102886-5.00010-4 (T.M.B.T.-F.E. (Third E. Letcher (Ed.)).
[4] H. Al-Sheeha, M. Marafi, V. Raghavan, M.S. Rana, Recycling and recovery routes for spent hydroprocessing catalyst waste, Ind. Eng. Chem. Res. 52 (2013) 12794–12801, https://doi.org/10.1021/ie4019148.
[5] S.K. Maity, E. Blanco, J. Ancheyta, F. Alonso, H. Fukuyama, Early stage deactivation of heavy crude oil hydroprocessing catalysts, Fuel 100 (2012) 17–23, https://doi.org/10.1126/science.181.4099.547.
[6] R.B. Levy, M. Boudart, Platinum-like behavior of tungsten carbide in surface catalysis, Sci. (80-.) 181 (1973) 547–549, https://doi.org/10.1126/science.181.4099.547.
[7] L. Volpe, M. Boudart, Compounds of molybdenum and tungsten with high specific surface area: II. Carbides, J. Solid State Chem. 59 (1985) 348–356, https://doi.org/10.1016/0022-4596(85)90302-0.
[8] L. Volpe, M. Boudart, Compounds of molybdenum and tungsten with high specific surface area: I. Nitrides, J. Solid State Chem. 59 (1985) 332–347, https://doi.org/10.1016/0022-4596(85)90301-9.
[9] J.S. Lee, L. Volpe, F.H. Ribeiro, M. Boudart, Molybdenum carbide catalysts: II. Topotactic synthesis of unsupported powders, J. Catal. 112 (1988) 44–53, https://doi.org/10.1016/0021-9517(88)90119-4.
[10] M.S. Rana, M.L. Huidobro, J. Ancheyta, M.T. Gomez, Effect of support composition on hydrogenolysis of thiophene and Maya crude, Catal. Today 107–108 (2005) 346–354, https://doi.org/10.1016/j.cattod.2005.07.029.
[11] J.N.R. Olvera, G.J. Gutiérrez, J.A.R. Serrano, A.M. Ovando, V.G. Febles, L.D. B. Arceo, Use of unsupported, mechanically alloyed NiWMoC nanocatalyst to reduce the viscosity of aquathermolysis reaction of heavy oil, Catal. Commun. 43 (2014) 131–135, https://doi.org/10.1016/j.catcom.2013.09.027.
[12] C.C. Yu, S. Ramanathan, F. Sherif, S.T. Oyama, Structural, surface, and catalytic properties of a new bimetallic V-Mo oxynitride catalyst for hydrodenitrogenation, J. Phys. Chem. 98 (1994) 13038–13041, https://doi.org/10.1021/j100100a036.
[13] S.T. Oyama, The Chemistry of Transition Metal Carbides and Nitrides, Springer Netherlands, Glasgow, 1996.
[14] J.C. Schlatter, S.T. Oyama, J.E. Metcalfe, J.M. Lambert, Catalytic behavior of selected transition metal carbides, nitrides, and borides in the hydrodenitrogenation of quinoline, Ind. Eng. Chem. Res. 27 (1988) 1648–1653, https://doi.org/10.1021/ie00081a014.
[15] J.G. Chen, Carbide and nitride overlayers on early transition metal surfaces: preparation, characterization, and reactivities, Chem. Rev. 96 (1996) 1477–1498, https://doi.org/10.1021/cr950232u.
[16] A.L. Stottlemyer, T.G. Kelly, Q. Meng, J.G. Chen, Reactions of oxygen-containing molecules on transition metal carbides: Surface science insight into potential applications in catalysis and electrocatalysis, Surf. Sci. Rep. 67 (2012) 201–232, https://doi.org/10.1016/j.surfrep.2012.07.001.
[17] E. Furimsky, Metal carbides and nitrides as potential catalysts for hydroprocessing, Appl. Catal. A Gen. 240 (2003) 1–28, https://doi.org/10.1016/S0926-860X(02)00428-3.
[18] L.A. Santillán-Vallejo, J.A. Melo-Banda, A.I. Reyes de la Torre, G. Sandoval-Robles, J.M. Domínguez, A. Montesinos-Castellanos, J.A. de los Reyes-Heredia, Supported (NiMo,CoMo)-carbide, -nitride phases: Effect of atomic ratios and phosphorus concentration on the HDS of thiophene and dibenzothiophene, Catal. Today 109 (2005) 33–41, https://doi.org/10.1016/j.cattod.2005.08.022.
[19] P.A. Aegerter, W.W.C. Quigley, G.J. Simpson, D.D. Ziegler, J.W. Logan, K. R. McCrea, S. Glazier, M.E. Bussell, Thiophene hydrodesulfurization over alumina-supported molybdenum carbide and nitride catalysts: adsorption sites, catalytic activities, and nature of the active surface, J. Catal. 164 (1996) 109–121.

[20] S.-K. Ihm, D.-W. Kim, D.-K. Lee, Effects of sulfidation of Mo nitride and CoMo nitride catalysts on thiophene HDS, in: C.H. Bartholomew, G.A. Fuentes (Eds.), Stud. Surf. Sci. Catal., Elsevier, 1997, pp. 343–350, https://doi.org/10.1016/S0167-2991(97)80173-5.
[21] S. Ramanathan, S.T. Oyama, New catalysts for hydroprocessing: transition metal carbides and nitrides, J. Phys. Chem. 99 (1995) 16365–16372, https://doi.org/10.1021/j100044a025.
[22] G.M. Dolce, P.E. Savage, L.T. Thompson, Hydrotreatment activities of supported molybdenum nitrides and carbides, Energy Fuels 11 (1997) 668–675, https://doi.org/10.1021/ef960083y.
[23] Y. Villasana, F.J. Méndez, M. Luis-Luis, J.L. Brito, Pollutant reduction and catalytic upgrading of a Venezuelan extra-heavy crude oil with Al2O3-supported NiW catalysts: effect of carburization, nitridation and sulfurization, Fuel 235 (2019) 577–588, https://doi.org/10.1016/j.fuel.2018.08.047.
[24] Y. Villasana, Y. Escalante, J.E. Rodríguez Nuñez, F.J. Méndez, S. Ramírez, M.Á. Luis-Luis, E. Cañizales, J. Ancheyta, J.L. Brito, Maya crude oil hydrotreating reaction in a batch reactor using alumina-supported NiMo carbide and nitride as catalysts, Catal. Today 220 (2014) 318–326, https://doi.org/10.1016/j.cattod.2013.10.025.
[25] ICDD, International Center for Diffraction Data, PCPDFWIN v.2.02. PDF-2 Data Base, Newtown Philadelphia, 1995.
[26] M.E. Bussell, P. Mills, B.P. Woodruff, R. Main, D.C. Phillips, Synthesis, characterization and evaluation of bimetallic/promoted carbides and nitrides for hydrodesulfurization catalysis, Am. Chem. Soc. Div. Pet. Chem. Prepr. (1999) 206–208.
[27] P. Da Costa, J.-M. Manoli, C. Potvin, G. Djéga-Mariadassou, Deep HDS on doped molybdenum carbides: From probe molecules to real feedstocks, Catal. Today 107–108 (2005) 520–530, https://doi.org/10.1016/j.cattod.2005.07.166.
[28] B. Diaz, S.J. Sawhill, D.H. Bale, R. Main, D.C. Phillips, S. Korlann, R. Self, M. E. Bussell, Hydrodesulfurization over supported monometallic, bimetallic and promoted carbide and nitride catalysts, Catal. Today 86 (2003) 191–209, https://doi.org/10.1016/S0920-5861(03)00411-5.
[29] J.M. Manoli, P. Da Costa, M. Brun, M. Vrinat, F. Maugé, C. Potvin, Hydrodesulfurization of 4,6-dimethyldibenzothiophene over promoted (Ni,P) alumina-supported molybdenum carbide catalysts: Activity and characterization of active sites, J. Catal. 221 (2004) 365–377, https://doi.org/10.1016/j.jcat.2003.08.011.
[30] V. Sundaramurthy, A.K. Dalai, J. Adjaye, HDN and HDS of different gas oils derived from Athabasca bitumen over phosphorus-doped NiMo/γ-Al2O3 carbides, Appl. Catal. B Environ. 68 (2006) 38–48, https://doi.org/10.1016/j.apcatb.2006.07.014.
[31] L. Brewer, A most striking confirmation of the Engel metallic correlation, Acta Met. 15 (1967) 553–556, https://doi.org/10.1016/0001-6160(67)90088-0.
[32] N. Engel, Copper, copper alloys and the electron concentration concept, Acta Met. 15 (1967) 557–563, https://doi.org/10.1016/0001-6160(67)90089-2.
[33] S. Lobos, R. Ravelo, J. Lazo, J.L. Brito, Síntesis y caracterización de nitruros bimetálicos, Actas XVI Encuentro Nac. Cat. álisis, Maracaibo, Venez. (2001).
[34] C. González, D. Posada, Efecto del {Hierro} como promotor en los catalizadores derivados de complejos tipo tiomolibdato para procesos de hidrodesulfuración, Venezuela, Universidad Nacional Experimental Politécnica, 1999.
[35] Y. Villasana, F. Ruscio-Vanalesti, C. Pfaff, F.J. Méndez, M.Á. Luis-Luis, J.L. Brito, Atomic ratio effect on catalytic performance of FeW-based carbides and nitrides on thiophene hydrodesulfurization, Fuel 110 (2013) 259–267, https://doi.org/10.1016/j.fuel.2012.11.055.
[36] H. Ge, X.-D. Wen, M.A. Ramos, R.R. Chianelli, S. Wang, J. Wang, Z. Qin, Z. Lyu, X. Li, Carbonization of ethylenediamine coimpregnated CoMo/Al2O3 catalysts sulfided by organic sulfiding agent, ACS Catal. 4 (2014) 2556–2565, https://doi.org/10.1021/cs500477x.
[37] M. Ramos, D. Ferrer, E. Martinez-Soto, H. Lopez-Lippmann, B. Torres, G. Berhault, R.R. Chianelli, In-situ HRTEM study of the reactive carbide phase of Co/MoS2 catalyst, Ultramicroscopy 127 (2013) 64–69, https://doi.org/10.1016/j.ultramic.2012.07.012.
[38] J.L. Brito, A.L. Barbosa, Effect of phase composition of the oxidic precursor on the HDS activity of the sulfided molybdates of Fe(II), Co(II), and Ni(II), J. Catal. 171 (1997) 467–475, https://doi.org/10.1006/jcat.1997.1796.
[39] M.A. Luis, A. Rives, R. Hubaut, B.P. Embaid, F. Gonzalez-Jimenez, C.E. Scott, HDS of dibenzothiophene and vanadyl porphyrin HDP on bulk Fe-Mo mixed sulphides, in: G.F.F.B. Delmon, P. Grange (Eds.), Stud. Surf. Sci. Catal., Elsevier, 1999, pp. 203–210, https://doi.org/10.1016/S0167-2991(99)80410-8.
[40] R. Hubaut, J. Altafulla, A. Rives, C. Scott, Characterization and HDS activities of mixed Fe–Mo sulphides supported on alumina and carbon, Fuel 86 (2007) 743–749, https://doi.org/10.1016/j.fuel.2006.09.012.
[41] Y. Villasana, S. Ramírez, J. Ancheyta, J.L. Brito, Effect of hydrotreating reaction conditions on viscosity, API gravity and specific gravity of maya crude oil, in: L.D. G. Sigalotti, J. Klapp, E. Sira (Eds.), Comput. Exp. Fluid Mech. with Appl. to Physics, Eng. Environ., Springer International Publishing, 2014, pp. 423–430, https://doi.org/10.1007/978-3-319-00191-3_28.
[42] Y. Villasana, Y. Escalante, J.E. Rodríguez Nuñez, F.J. Méndez, S. Ramírez, M.Á. Luis-Luis, E. Cañizales, J. Ancheyta, J.L. Brito, Maya crude oil hydrotreating reaction in a batch reactor using alumina-supported NiMo carbide and nitride as catalysts, Catal. Today 220–222 (2014) 318–326, https://doi.org/10.1016/j.cattod.2013.10.025.
[43] C. GALARRAGA, A stable catalyst for heavy oil processing II. Preparation and characterization, J. Catal. 134 (1992) 98–106, https://doi.org/10.1016/0021-9517(92)90213-2.
[44] M.M. Ramirez de Agudelo, C. Galarraga, A stable catalyst for heavy oil processing, Chem. Eng. J. 46 (1991) 61–68, https://doi.org/10.1016/0300-9467(91)80024-Q.
[45] C. Leyva, J. Ancheyta, G. Centeno, Effect of alumina and silica–alumina supported NiMo catalysts on the properties of asphaltenes during hydroprocessing of heavy petroleum, Fuel 138 (2014) 111–117, https://doi.org/10.1016/j.fuel.2014.08.023.
[46] S. Acevedo, J.M. Cordero, H. Carrier, B. Bouyssiere, R. Lobinski, Trapping of paraffin and other compounds by asphaltenes detected by laser desorption ionization−time of flight mass spectrometry (LDI−TOF MS): role of A1 and A2 asphaltene fractions in this trapping, Energy Fuels 23 (2009) 842–848, https://doi.org/10.1021/ef8007745.
[47] H. Zhang, G. Chen, L. Bai, N. Chang, Y. Wang, Selective hydrogenation of aromatics in coal-derived liquids over novel NiW and NiMo carbide catalysts, Fuel 244 (2019) 359–365, https://doi.org/10.1016/j.fuel.2019.02.015.
[48] M. Nagai, Transition-metal nitrides for hydrotreating catalyst—synthesis, surface properties, and reactivities, Appl. Catal. A Gen. 322 (2007) 178–190, https://doi.org/10.1016/j.apcata.2007.01.006.
[49] E. Puello-Polo, J.L. Brito, Effect of the type of precursor and the synthesis method on thiophene hydrodesulfurization activity of activated carbon supported Fe-Mo, Co-Mo and Ni-Mo carbides, J. Mol. Catal. A Chem. 281 (2008) 85–92, https://doi.org/10.1016/j.molcata.2007.09.015.
[50] E. Puello-Polo, A. Gutiérrez-Alejandre, G. González, J.L. Brito, Relationship between sulfidation and HDS catalytic activity of activated carbon supported Mo, Fe–Mo, Co–Mo and Ni–Mo carbides, Catal. Lett. 135 (2010) 212–218, https://doi.org/10.1007/s10562-010-0303-6.
[51] P.J. Mangnus, A. Riezebos, A.D. Vanlangeveld, J.A. Moulijn, Temperature-programmed reduction and HDS activity of sulfided transition metal catalysts: formation of nonstoichiometric sulfur, J. Catal. 151 (1995) 178–191, https://doi.org/10.1006/jcat.1995.1020.
[52] B. Scheffer, N.J.J. Dekker, P.J. Mangnus, J.A. Moulijn, A temperature-programmed reduction study of sulfided CoMo/Al2O3 hydrodesulfurization catalysts, J. Catal. 121 (1990) 31–46, https://doi.org/10.1016/0021-9517(90)90214-5.